Stricker and Weygand
Journal of Materials Science: Materials Theory (2024) 8:12
https://doi.org/10.1186/s41313-024-00065-7

Journal of Materials Science: Materials Theory

RESEARCH Open Access

A model for physical dislocation transmission through grain boundaries and its implementation in a discrete dislocation dynamics tool

M. Stricker[1*] and D. Weygand[2]

*Correspondence:
markus.stricker@rub.de

[1] Interdisciplinary Centre for Advanced Materials Simulation, Ruhr-Universität Bochum, Universitätsstraße 150, 44801 Bochum, Germany
[2] Institute for Applied Materials, Karlsruhe Institute of Technology, Kaiserstraße 12, 76131 Karlsruhe, Germany

Abstract

The mechanical behavior of most metals in engineering applications is dominated by the grain size. Physics-based models of the interaction between dislocations and the grain boundary are important to correctly predict the plastic deformation behavior of polycrystalline materials. Dislocation-grain boundary interaction is complex and a challenge to model. We present a model for simulating the physical transmission of dislocations through grain boundaries within Discrete Dislocation Dynamics tools. The properties (glide plane, Burgers vector, initial length) of the transmitted dislocation are chosen based on geometric criteria as well as a maximization of the resolved shear stress of the transmitted dislocation. Additionally, stress and displacement transparency as well as the discontinuity are ensured via a grain boundary dislocation – a butterfly-like geometry in the general case – whose properties are selected to minimize the residual Burgers vector at the interface. This additional 'grain boundary dislocation' allows a direct comparison as well as a calibration of the model with experiments on the macroscale particularly for neighboring grains with a high dislocation density contrast. Two basic examples illustrate the model and an application to a 40-grain polycrystal demonstrates the scalability of the approach.

Keywords: Dislocations, Grain boundaries, Transmission, Discrete Dislocation Dynamics

Introduction

Grain boundaries are the dominating crystal defects for the mechanical behavior of most engineering materials. Their nature and distribution defines the deformation behavior of almost all metallic components in practice because most of them are polycrystals. The most important property to predict macroscopic mechanical behavior is the grain size which limits the motion of dislocations in an otherwise perfect crystal. This behavior was cast into a law known as the Hall-Petch relationship (Hall 1951; Petch 1953). It states that the flow stress scales inversely with the square root of the grain size. The underlying assumption is that grain boundaries are, in a first approximation, barriers for

dislocations. When dislocation motion is obstructed, they pile up at obstacles and the outcome is a size effect: smaller grains lead to higher yield strength. While this assumption is a good first approximation, a consequence of the pile-up is that the stresses at the grain boundary can become very large. 'Very large' means that the stress at the head of the pile-up is the applied stress magnified by the number of dislocations in the pile-up (Hull and Bacon 2011).

With a large stress, the probability for the dislocation to overcome the grain boundary as an obstacle increases, e.g. by nucleating dislocations from the grain boundary. A plasticity model that accurately describes the behavior of polycrystals consequently has to take into account how dislocations interact with grain boundaries. Dislocation-grain boundary interaction includes i) obstruction and ii) transmission or partial transmission with a residual Burgers vector. Criteria for transmission and prediction of the active outgoing slip system include a geometric condition, a resolved shear stress condition, as well as a residual grain boundary dislocation condition (Lee et al. 1989). The first states that the angle between the intersection of the incoming and the outgoing dislocation should be minimized. The second states that the prediction for the outgoing slip system should maximize the resolved shear stress. The third states that the residual Burgers vector, determined by the difference of the incoming and outgoing dislocations, should be minimized.

In modeling, this can be cast into effective models (Quek et al. 2014; Stricker et al. 2015) or treated explicitly (Quek et al. 2014; Kumar et al. 2010; Zhou and LeSar 2012a, b; Gao et al. 2011). *Effective model* means that there is no physical transmission of dislocations but the superposition of the stress and displacement fields of the dislocations which pile up left and right of the grain boundary can be interpreted as *effective* transmission because the superposed fields are indistinguishable from physical transmission, cf. Stricker et al. (2015). The downside of effective models is that large dislocation density contrasts, i.e. two grains – one dislocation-free and the other with dislocations – will not behave physically correct when subjected to load because only one grain will display a pile-up and this pile-up has no appropriate counterpart on the other side of the grain boundary to partially or fully cancel out depending on the misorientation.

Existing models for transmission in discrete dislocation dynamics frameworks are either two-dimensional (Kumar et al. 2010; Quek et al. 2014, 2015) or special cases of no (Zhou and LeSar 2012a, b) or low (Burbery et al. 2017) misorientations between grains or are coupled to molecular dynamics (Gao et al. 2011). Models which concentrate on specific cases are, naturally, limited in their broader application. The focus on specific misorientation cases has its reasons because there are several challenges in developing a general model for transmission. Two *general* three-dimensional implementations exist for discrete dislocation dynamics frameworks. One (Zhang et al. 2021) is a coarse-graining technique to deal with multiple absorption events and also uses coarse-grained grain boundaries as a source for dislocation emission which we will not discuss in detail here because the approach is very different. The other model (Cho et al. 2020), closer to our proposition, is a model based on the concept of a grain boundary dislocation allowing to model the general and complex interactions with arbitrary grain boundaries: absorption, motion, and emission of dislocations at, in, and from grain boundaries, based on Koning et al. (2002). They use the

concept of grain boundary nodes. Such nodes are associated with both grains which share a grain boundary. From the definition of grain boundary nodes follows a second concept: grain boundary segments to denote segments whose both ending nodes are grain boundary nodes. From nodes and segments follows the definition of a dislocation, a set of connected segments. In case of transmission (or rather *emission* as per (Cho et al. 2020)), a residual dislocation may be placed together with the outgoing dislocation and the grain boundary dislocation can move inside the grain boundary. The latter is physically possible, but in Cho et al. (2020) no special explanation is given about the mobility law for such a grain boundary segment. In addition, no residual dislocation for the incoming dislocation is foreseen. Decomposition of the Burgers vector of the incoming dislocation to a residual and a grain boundary Burgers vector as reported in Dewald and Curtin (2011) are also not foreseen. Further, following their definitions, a single dislocation can start with segments in one grain, followed by grain boundary segments, and then *leave* the grain boundary again into the first grain with regular segments or end in a residual dislocation.

Challenges for a general model include that grain boundaries have to be transparent to the stress field of dislocations to either side of it (Stricker et al. 2015). *Transparency* here means that dislocations in one grain interact with dislocations in every other grain. This is usually inherent to the method with the usual approaches but requires additional care with more advanced superposition schemes as in O'day and Curtin (2004). Anisotropic elasticity shows that the energy of a dislocation near and far from a grain boundary is different which leads to repulsive or attractive image forces (Barnett and Lothe 1974). The origin of the image stress is the rotation of the two neighboring grains and can be of the magnitude of shear stress to initiate glide. On the atomic scale, a dislocation can enter a grain boundary since it is usually not an infinitesimally thin entity, with the consequence that the dislocation-grain boundary interaction results in changes of atomic arrangements. Direct atomistic modeling of grain boundaries is not possible in a discrete dislocation dynamics (DDD) framework. However, some physical aspects can be considered for a useful approximation:

- Dislocation nucleation: a step introduced by an incoming dislocation is sent back into both grains
- Grain boundary sliding
- Grain boundary cracking
- Delocalization by smearing out the Burgers vector to smoothen the step

Out of those, our model includes transmission, reflection, and delocalization. It is based on experimental findings and geometrical considerations. Our model is valid for arbitrary grain boundaries and can also be extended to include different crystal systems like an fcc/bcc interface. Here, we focus on the first steps of validating the model. Calibration and comparison to experiments on the micrometer scale (Imrich et al. 2014; Malyar et al. 2019) are planned for future work. Our model is based on three criteria: the minimization of the angle between the incoming and outgoing glide planes, the maximization of the resolved shear stress on the outgoing system and the minimization of the residual Burgers vector.

The paper is organized as follows: The "Model" section introduces the proposed model in detail including aspects of the implementation. The "Results" section shows the results for a bicrystal with an *artificial* grain boundary (no misorientation) with one incoming glide system. The second example is a generic tilt/twist grain boundary with one incoming glide system. We close with the presentation of the mechanical response for a polycrystal with 40 grains with and without our transmission model. The "Discussion" section discusses the results as well as the validity of the model. And, finally, the "Conclusion" section provides a brief summary and a strategy how the model can be calibrated against experimental evidence.

Model

In the following, we present a model for three-dimensional discrete dislocation transmission through planar grain boundaries based on a reduced parameter set accouting for the displacement discontinuity at the grain boundary and including stress and displacement transparency. Deliberations on a suitable parameter set can be inferred e.g. by looking at grain boundary modeling in continuum theories (Gottschalk et al. 2015). Dislocations are either directly transmitted, transmitted with a residual Burgers vector, or they just stay at the grain boundary with their associated stresses (Sutton and Balluffi 1996). The parameter set includes the crystallographic definition of the grain boundary including the participating Burgers vectors and glide plane normals of the specific event and the stress state. This set can in principle be extended to account for a dependence on temperature, time, and strain rate (Malyar et al. 2018).

A grain boundary is described by five macroscopic parameters which define the interface between the crystals (Sutton and Balluffi 1996), the angle and the axis of misorientations, and the normal vector of the grain boundary plane. This defines the crystallography and, therefore, the geometric relationship between the glide systems of the two neighboring crystals. For the implementation within DDD, we restrict ourselves to flat grain boundaries. The translational degree of freedom between the two grains would add three more parameters, which are generally disregarded. Those degrees might be important for low Σ grain boundaries like twin boundaries, where a slight translational offset may disturb matching glide systems.

Interface dislocation: butterfly geometry

Apart from the geometry, the most important ingredient of a transmission model is the prediction of the glide system of the outgoing dislocation. Several geometrical criteria have been proposed based on experimental observations (Livingston and Chalmers 1957; Lagow et al. 2001; Guo et al. 2014; Kacher et al. 2014). One missing ingredient in earlier approaches is the resolved shear stress, which was rectified by Shen et al. (1986). We adopt the prediction of the transmitted dislocation based on Lee et al. (1989), consisting of three event criteria for each individual event:

1. Minimization of the angle between the incoming and outgoing glide planes.
2. Maximization of the shear stress on the outgoing system induced by the incoming system.
3. Minimization of the residual Burgers vector.

Minimizations of the glide plane normal differences and residual Burgers vectors are done using the L2 norm. Maximization of the shear stress is based on the local stress state. These three criteria have also been rationalized based on molecular dynamics simulations (Spearot and Sangid 2014; Bieler et al. 2014). The choice of the outgoing dislocation is important because – depending on the system – it can be the dominant feature controlling the macroscopic response (Burbery et al. 2014). The novelty of our model is an additional 'grain boundary dislocation' to minimize the effect of the differences of the stress fields of the incoming and outgoing dislocations. This mimics an atomic dislocation transmission; the incoming and outgoing dislocations are connected with a butterfly-shaped grain boundary dislocation schematically shown in Fig. 1.

Once an incoming dislocation (green, subscript 1) approaches the grain boundary, the dislocation aligns with an increasingly long section parallel to the grain boundary plane. Among those aligned dislocation segments, a candidate section for transmission through the grain boundary is determined. The length of the section has to exceed l_{crit} which is chosen to be in the range of $100 - 200\,a$, where a is the lattice constant. Results shown later do not critically depend on the precise value. Subsequently, a minimization of the

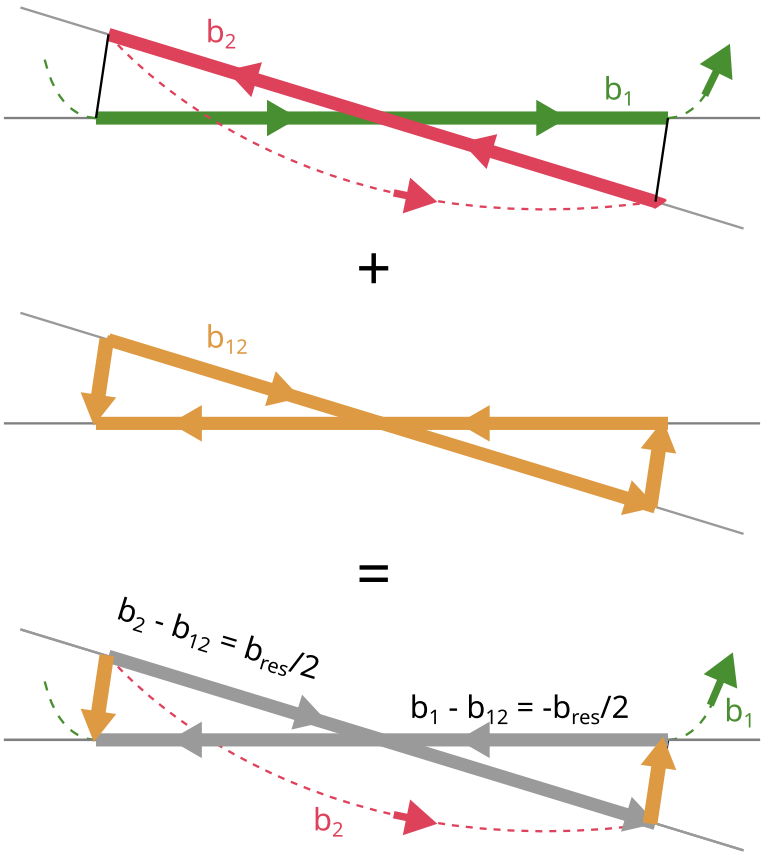

Fig. 1 Sketch of the butterfly-shaped interface dislocation: Light gray lines indicate the intersection line of the incoming and outgoing glide planes. View is normal to the grain boundary plane. The grain boundary butterfly-shaped dislocation (orange; Burgers vector indicated with subscript 12) connects the incoming (green; subscript 1) and outgoing dislocation (red; subscript 2). Superposition of incoming, outgoing, and interface dislocation results in a residual Burgers vector (gray; subscript *res*) which stays in the grain boundary plane. Colored arrows along the dislocation sections indicate the line direction of the dislocation

outgoing glide plane normal and Burgers vector with respect to the incoming is performed. This determines the plane $\mathbf{n}_2$ and the Burgers vector $\mathbf{b}_2$ of the outgoing dislocation (red, subscript 2). The Burgers vector of the grain boundary dislocation is given by $\mathbf{b}_{12} = \frac{1}{2}(\mathbf{b}_1 + \mathbf{b}_2)$.

Both dislocations with all of their segments stay as their are but, in addition, we place a grain boundary dislocation in the shape of a butterfly (orange) for the general case in between them. The orange segments in Fig. 1 center affect the incoming and outgoing dislocations (Fig. 1, top), the two connecting segments in orange (Fig. 1 bottom) constitute the residual effect of the transmission event. The nodes from the grain boundary dislocation are in addition to and independent of the incoming and outgoing dislocations, i.e. no node or segment is shared between the three dislocations. Nodes belonging to this connection are treated similar to a dislocation junction, i.e. the end-nodes of the "interface reactions" are only allowed to move along the junction line direction. Thus the superposition of the incoming aligned dislocation section with the grain boundary dislocation the residual Burgers vector of the interface reaction in the first grain becomes $\frac{1}{2}\mathbf{b}_{\text{res}} = \mathbf{b}_{12} - \mathbf{b}_1$. On the outgoing plane superposition results in $\frac{1}{2}\mathbf{b}_{\text{res}} = \mathbf{b}_2 - \mathbf{b}_{12}$. A topologically correct closure of the grain boundary dislocation is ensured with sections of Burgers vector $\mathbf{b}_{12}$. The butterfly construct may generate compressive and tensile stresses at the grain boundary which aid the relaxation and ensures the correct displacement discontinuity. It allows to model a step along the trace of the incoming and the transmitted dislocation. Comparing the elastic energy of the residual dislocations without interaction among each other, the two *traces* each with $\frac{1}{2}\mathbf{b}_{\text{res}}$ and length l have a lower total elastic energy as compared to one trace with $\mathbf{b}_{\text{res}}$ and length l. In addition to Cho et al. (2020), the butterfly grain boundary dislocation approach allows to include a general dissociation of the incoming Burgers vector to a residual and a grain boundary Burgers vector, cf. Dewald and Curtin (2011).

Since the grain boundary dislocation's Burgers vector $\mathbf{b}_{12}$ may not be within the grain boundary plane and the butterfly loop may have interstitial character, the motion of the the closing sections with Burgers vector $\mathbf{b}_{12}$ may (physically) require diffusion within the grain boundary. This introduces a temperature dependency of the expansion of the butterfly loop and thus for the whole transmission/nucleation process.

Our proposed model is implemented in an existing discrete dislocation dynamics framework (Weygand et al. 2002; Weygand and Gumbsch 2005; Weygand et al. 2009) and extends the polycrystal simulation capabilities already existing in the code based on *effective* transmission (Zhang et al. 2014; Stricker et al. 2015; Bayerschen et al. 2015). Dislocations are tested for transmission once during a global time step, where the boundary conditions for the elastic part of our DDD framework (Weygand et al. 2002) are updated. The dislocation structure is evolved with a sub-time step of about $1 - 5 \times 10^{-13}s$ which is about two orders of magnitude smaller than the global time step. For each dislocation, the following tests are carried out to identify dislocation sections as candidates for transmission events:

```
if aligned section of length ℓ ≥ ℓ_crit exist then
  if not junction then
    determine distance d of section from grain boundary
    if d ≤ d_crit then
      Dislocation sector is straightened for possible transmission
      if Transmission condition fulfilled then
        perform transmission
      end if
    end if
  end if
end if
```

where l_{crit} is a critical length and d_{crit} is a critical distance of the order of b. In case of a pile-up configuration, we ensure that only the leading dislocation is tested.

Subsequently, a suitable glide system in the neighboring grain is identified for the transmitted dislocation. This choice is based on minimizing the difference in glide plane normals and the residual Burgers vector. If these criteria do not yield a unique geometric solution, the outgoing glide system with the highest resolved shear stress is chosen.

A butterfly-shaped grain boundary dislocation (Fig. 1) is constructed such that the incoming and outgoing sections overlap with sections of the grain boundary dislocation, effectively canceling parts of the grain boundary steps on both sides. Further, the connections between the dislocation nodes are made with the section of the grain boundary dislocation with Burgers vector $\mathbf{b}_{12}$. This grain boundary dislocation can, in the general case, not move without additional assumptions. Because in the general case, its Burgers vector is not contained within the 6 fcc lattice Burgers vectors and its motion may involve grain boundary diffusion.

The physical interpretation of the butterfly dislocation can be rationalized as follows: By decomposing the Burgers vector in a normal and tangential (with respect to the orientation of the grain boundary) part $\mathbf{b}_{12} = \mathbf{b}_{12,\mathrm{n}} + \mathbf{b}_{12,\mathrm{t}}$, the dislocation can be interpreted as a superposition of two contributions from incoming and outgoing dislocations. The normal (sessile) component can be interpreted as an interstitial/vacancy dislocation, whereas the tangential component as a glissile dislocation.

The glissile component of the butterfly dislocation enables the transmission of strain by the trace misfit dislocation in the boundary plane. In effect, it facilitates the transmission process. The sessile component of the butterfly dislocation also enables the transmission of strain across the grain boundary, a step. Effectively creating an alternating tension-compression state, the *butterfly* dislocation can be interpreted as a combined vacancy-interstitional dislocation, allowing the relaxation of the boundary. Physically, shrinking or growing of such an interfacial dislocation is material transfer from the vacancy to the interstitial side and can be interpreted as climb. This implies that a future refinement of the model should consider thermal activation. Here, we only present the first step to include a grain boundary dislocation, a temperature dependency is not included. Note, the interaction between the incoming and outgoing dislocations is purely via their respective stress fields and the grain boundary dislocation. The motion

of individual nodes limiting the interface junction is not forcefully (numerically) linked between the dislocations, e.g. relevant for the scenario of zero misorientation in the Results section.

To illustrate the effect on the stress and displacement fields of this butterfly construct, we refer the reader to "Bicrystal with generic grain boundary" section, Fig. 6, where we present and discuss the respective fields for σ_{xx} and u_x for a generic grain boundary. In addition, we present a modified version of our butterfly that mimics the approach taken in Cho et al. (2020) and illustrate the differences in detail.

Stress calculation: butterfly dislocations

Interfaces, resp. grain boundaries, have different abilities to relax the stress/displacement jumps introduced by in- and outgoing dislocations, depending on their misorientation and thus local atomic structure. Consider two extremes: In case of a twin boundary, little relaxation is possible and mainly screw dislocation may cross the twin boundaries (Jin et al. 2008) or in case of a non-screw dislocation, well-defined glissile Shockley partial dislocations may be left as residual interface dislocation (Jin et al. 2008). In such a case, the full stress field should be included in the interaction calculation. Thus, e.g. for Σ boundaries, it seems reasonable to take the full stress field of the butterfly interface dislocation into account. For general boundaries, atomic relaxation is possible and a localized well defined dislocation within the interface is no longer found. In this case, a large cutoff radius for regularized stress fields (Cai et al. 2006) may be used to effectively screen the stress fields of interface dislocation or the residual dislocation parts modeled here as junctions between the butterfly dislocation and the incoming resp. outgoing dislocation. In the other extreme case, the interface dislocations and junctions would not interact with the dislocation within the material at all.

In the examples shown, we assumed that the interface junctions have effectively no stress field, while the GB dislocation links which connect the two junctions have the full stress field. The consequences of this assumption is that the transmission occurs more easily as the residual dislocation would always attract the outgoing part: The transmission occurs at lower stresses for a fixed length l_{crit} or is only performed once the aligned sector length is larger for a given stress level. The stability of the transmission "test loop" is checked based on nodal forces which have to lead to further expansion of the latter. The transmission process may collapse if the environment is not favorable any more.

Results

For the validation and the effects on dislocation evolution of our model we first use two types of grain boundaries representing the two limits of misorientations: zero and a generic misorientation with tilt and twist components. Later, we present a polycrystal containing 40 grains simulated with and without transmission. Zero misorientation means that the two neighboring grains have the same crystallographic orientation and the grain boundary is just a numerical stop. The expected behavior of this system should be that of a single crystal spanning the entire simulated volume. Ideally, the transmission process which is governed by the parameters minimal length l_{crit} and d_{crit} for the aligned / to be transmitted dislocation should be indistinguishable from the case where no grain boundary is present. This example serves to demonstrate that the coupling between the

two lattice dislocations via the grain boundary dislocation works as intended. The second, generic case with combined tilt and twist misorientation demonstrates the effect of the butterfly and how the transmitted dislocation glides.

Both cases are initially populated with one dislocation source in the left grain whereas the right grain is dislocation free. Note, the *correct* simulation of these systems is impossible without explicit transmission of dislocations.

Bicrystal with artificial grain boundary

This case consists of two grains with the same orientation, i.e. no misorientation. A time-series of the evolution of the dislocation structure during a shear test is shown in Fig. 2.

The left grain includes an edge-type Frank-Read source with a Burgers vector along the x-direction. The system is subjected to shear loading in x-direction. First, the source bows out and upon reaching the grain boundary, dislocation motion is not inhibited by the grain boundary. The grain boundary is effectively invisible for the dislocation. Minimization of the glide system normals' difference and the residual Burgers vector is trivial here: the outgoing glide system is exactly the same as the incoming. Continuity of the motion of dislocations is ensured by stress interaction of the participating dislocations. No other criteria are necessary. None of the superimposed dislocation structures for different time steps (time step: t_i with $i = 1, ..., 4$) shown in Fig. 2 can be used to identify the system as a bicrystal. The shape of the dislocation through the orange line, indicating the grain boundary's position, is not significantly affected, although the dislocation left and right of the grain boundary are numerically different entities and only coupled via their stress fields.

Macroscopically, neither the dislocation density nor the stress evolution is discernible from single crystal behavior as shown in Fig. 3: When the stress reaches the critical level, a dislocation bows out completely, sweeps the whole length of the crystal and the

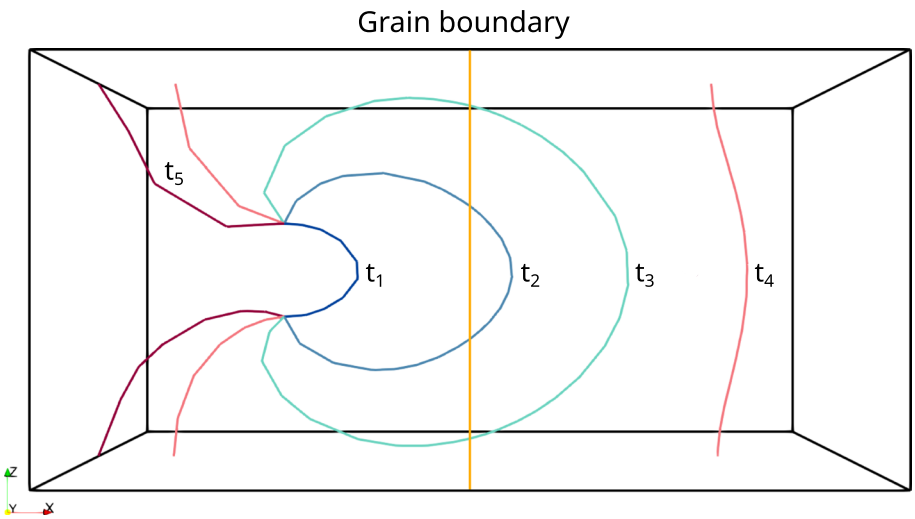

Fig. 2 Top view of a crystal with artificial grain boundary (no crystallographic misorientation) under shear load in x-direction; the orange line in the center is the (flat) grain boundary dislocation of time steps t_4 and t_5; several time steps t_1 to t_5 are overlaid showing the evolution of the dislocation as it is transmitted through the grain boundary (dark blue to dark red). The grain boundary is effectively invisible for the dislocation, as it should be

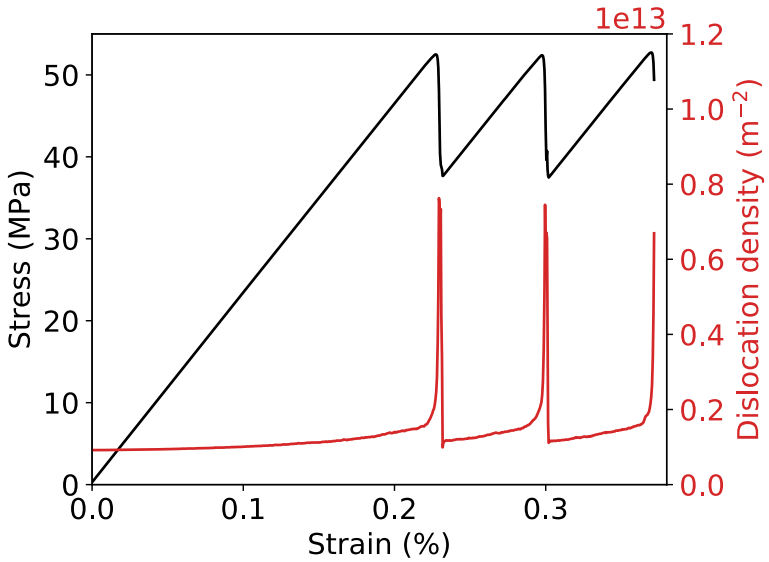

Fig. 3 Stress and dislocation density vs. strain for the bicrystal simulation without misorientaion shown in Fig. 2

dislocation density drops to the initial value showing no dislocation storage. The stress-strain curve shows no hardening, only the known *sawtooth* signature of a single operating Frank-Read source without obstacles and without resulting dislocation storage. Different peak heights in the dislocation density is attributed to slightly different bow-out behavior of the successive dislocations.

This example is important in the context of DDD since DDD is based on superposition. Our example shows a limiting case: large dislocation density contrast and no misorientation between grains. The grain boundary dislocation, however, is topologically a "collapsed" butterfly, but flat, i.e. schematically the red and green dislocations from Fig. 1 lie on top of each other without misorientation and the orange segments closing the interface dislocation in the bottom image have zero length. In essence, this example already validates our approach because the only difference to the general case is now the misorientation between the incoming and outgoing dislocation.

Bicrystal with generic grain boundary

The second example is a bicrystal with a misorientation of $\approx 38°$ (rotation axis $\approx [\bar{1}9\bar{5}]$) with tilt and twist components and shown in Fig. 4. Again, only one (the left) grain has an edge-type Frank-Read source on a glide plane with normal vector along the y axis of the laboratory frame while the other is dislocation free. The misorientation is chosen in a way that the incoming dislocation experiences a slightly larger resolved shear stress than the transmitted dislocation to stabilize the outgoing dislocation.

First, the Frank-Read source bows out (time step t_1, dark blue). Once the dislocation reaches the grain boundary (t_2, light blue), the algorithm chooses the outgoing plane by minimizing the difference between the incoming and outgoing normals as well as the Burgers vector and a new dislocation is introduced along with the grain boundary dislocation (butterfly construction). The grain boundary butterfly dislocation is shown in

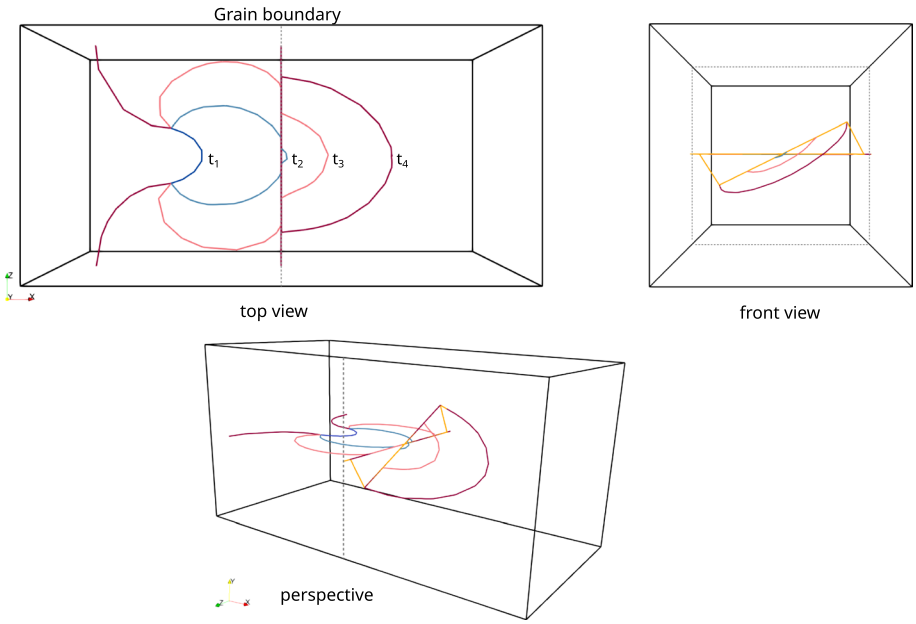

Fig. 4 Bicrystal with generic tilt and twist misorientation of ≈ 38° around a rotation axis ≈ $[\bar{1}9\bar{5}]$. Time steps t_1 through t_4 indicate the time series, each with a different color (blue to red); orange shows the grain boundary dislocation in the front and perspective view for time step t_4. The grey dashed line indicates the location of the grain boundary. The resolved shear stresses in both grains are such that the transmitted dislocation experiences a slightly smaller resolved shear stress

orange in the front and perspective views. Closing segments of the non-grain boundary dislocations are shown as residual dislocations – the incoming dislocation's residual lies horizontally flat at the grain boundary, the other tilted and twisted in accordance with the crystallographic orientation in the second grain. Once the Frank-Read source in the first grain is closed, it requires a comparatively larger stress to bow out again and the transmitted dislocation (t_4, red) expands and bows out instead.

Figure 5 shows the stress-strain and the dislocation density evolution for this example. After the first dislocation is emitted, work hardening is clearly visible because the next dislocation can not easily penetrate the grain boundary. In other words, the next emission results in temporary dislocation storage before the increase in applied shear stress is sufficiently large to overcome the backstress exerted by the interface dislocation before which results in the next transmission event.

Figure 6 shows the stress and displacement fields for the components σ_{xx} and u_x for the time step t_4 (see Fig. 4) for the individual contributions from the incoming dislocation, the outgoing dislocation, the butterfly construct, and their superposition. In addition, we present a modified version of the butterfly construct that mimics the approach taken in Ref. Cho et al. (2020). The stress fields of the incoming and outgoing dislocations alone are as expected (Fig. 6a, top row). The butterfly construct with the Burgers vector $\mathbf{b}_{12}$ (Fig. 6a, center left) shows the expected symmetry of compressive and tensile components in the two "wings", as $\mathbf{b}_{12}$ has a non-zero component along the x-axis in the sample frame. For this given misorientation of a general grain boundary, the summation of all three contributions show a significant canceling of the stress field along the grain boundary while the closing grain boundary dislocation

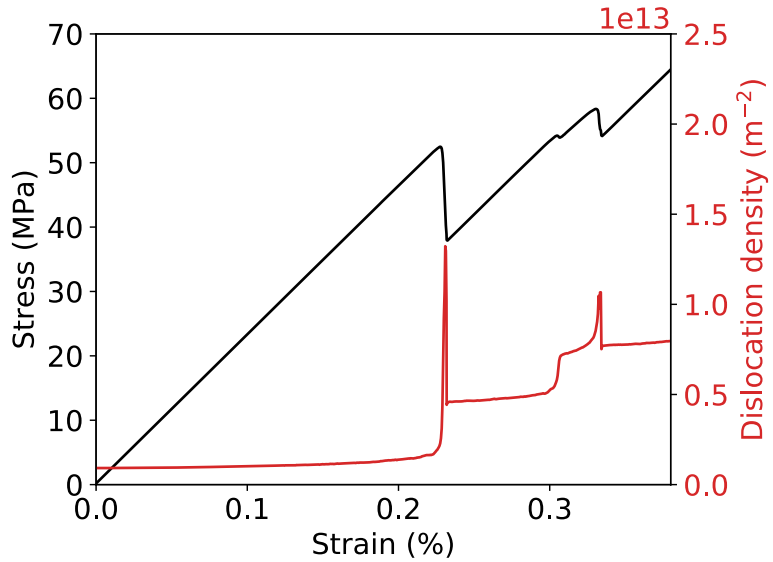

Fig. 5 Stress and dislocation density vs. strain for the simulation depicted in Fig. 4. Hardening is clearly visible

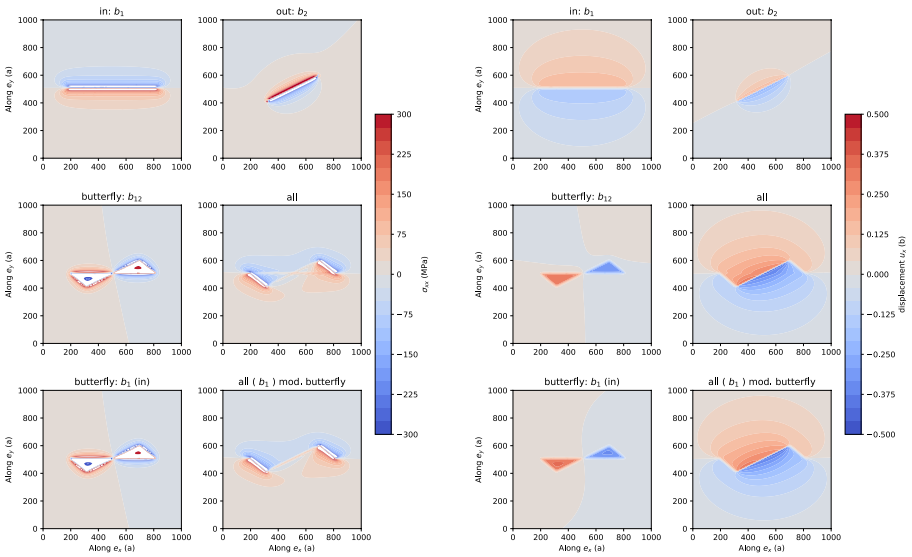

(a) Stress field contributions for component σ_{xx}. (b) Displacement field contributions for component u_x.

Fig. 6 Stress σ_{XX} (a) and displacement u_X (b) field contributions and superpositions evaluated on an x-y plane at a distance of 10 a from the grain boundary in grain 2 (cf. Fig. 4 for coordinate system) at time step t_4, where a is the lattice constant. We show the respective fields for the incoming dislocation (top left), outgoing dislocation (top right), the butterfly construct (center left) and their superposition (center right). In addition, we show a modified version of the butterfly construct that mimics the dislocation transmission as presented in Cho et al. (2020): bottom left shows the butterfly construct with b_1 and the modified superposition (bottom right)

links are clearly visible (Fig. 6a, center right). The approach taken in Ref. Cho et al. (2020) allows the motion of a grain boundary segment with Burgers vector $\mathbf{b}_1$ of the incoming plane and no residual dislocation is left at the intersection of the glide plane with the grain boundary of the incoming dislocation. In our scheme, this would

correspond to a butterfly dislocation with the Burgers vector $\mathbf{b}_1$. Figure 6a, bottom row, shows this scenario: a $\mathbf{b}_1$ butterfly dislocation and the superposition of all contributions. There, it is clearly visible that by construction no trace of the incoming dislocation is visible while a larger residual Burgers vector and its stress field is visible on the transmission side (compare Fig. 6a center right with bottom right panels), see also the corresponding displacement fields in the same arrangement in Fig. 6b.

In our current state of the butterfly model, we propose to use $\mathbf{b}_{12} = \frac{1}{2}(\mathbf{b}_1 + \mathbf{b}_2)$ which leaves a residual Burgers vector of $\mathbf{b}_\mathrm{r} = \pm\frac{1}{2}(\mathbf{b}_1 - \mathbf{b}_2)$ on both, the incoming and the outgoing side. The elastic energy of this construct is proportional to $\mathbf{b}_\mathrm{r}^2$. Neglecting the connecting links, the excess elastic energy of the butterfly construction is, therefore, halved compared to using $\mathbf{b}_\mathrm{r} = \mathbf{b}_1 - \mathbf{b}_2$. Since the perfect motion of a grain boundary dislocation with $\mathbf{b}_1$ without leaving a trace on the incoming side is unlikely, we propose to use a 'grain boundary dislocation' with average properties for modeling grain boundary transmission in a discrete dislocation dynamics framework. But this is open for debate: a different decomposition of the Burgers vector of the incoming dislocation seems plausible, e.g. derived through molecular dynamics simulations, which could also be used in the future.

Polycrystal with 40 grains

To illustrate the role of transmission of dislocations through grain boundaries on the overall mechanical behavior, a non-periodic cuboidal polycrystalline fcc sample with a side length of 8 μm is generated using a Voronoi scheme. The generated grain shapes are not further optimized to reflect realistic grains.

The crystallographic orientations of the grains are chosen at random. The initial dislocation structure consists of Frank-Read sources with source length between 0.8 μm and 1.5 μm. Each grain initially contains 8 dislocations which are randomly picked resulting in populating all 4 available glide planes with two sources. The initial dislocation density is $\rho \approx 10^{12}\mathrm{m}^{-2}$.

Subsequently, the sample is deformed in tension using a strain rate of $2000\mathrm{s}^{-1}$ by applying displacement boundary conditions on the top and bottom surface along the y-direction. Remaining surface degrees of freedom are traction free. In this example, we demonstrate two extreme cases starting from the same initial dislocation distribution: i) impenetrable vs. ii) penetrable grain boundaries allowing for dislocation transmission and perfect grain boundary relaxation. In the latter, the stress fields of residual grain boundary junctions are excluded while the interface dislocation links are included. The displacement field of the interface dislocation is taken into account for the update of the boundary conditions. The critical length l_{crit} is set to $200\,a$. These parameters maximize the number of transmission events and overestimate the softening effect by dislocation transmission substantially. Thus, transmission occurs once the stress on a "hypothetical" / test dislocation in the neighboring grain is large enough to allow for a (transmitted) dislocation to bow out.

Figure 7 shows the dislocation structures with transmission in a) and b) for 0.1 % and 0.18 % total strain. Interface dislocations are visible at the grain boundaries. An increase in total strain results in a drastic density increase of interface dislocations (junctions and links). Figure 7 c) shows the dislocation structure for impenetrable grain boundaries.

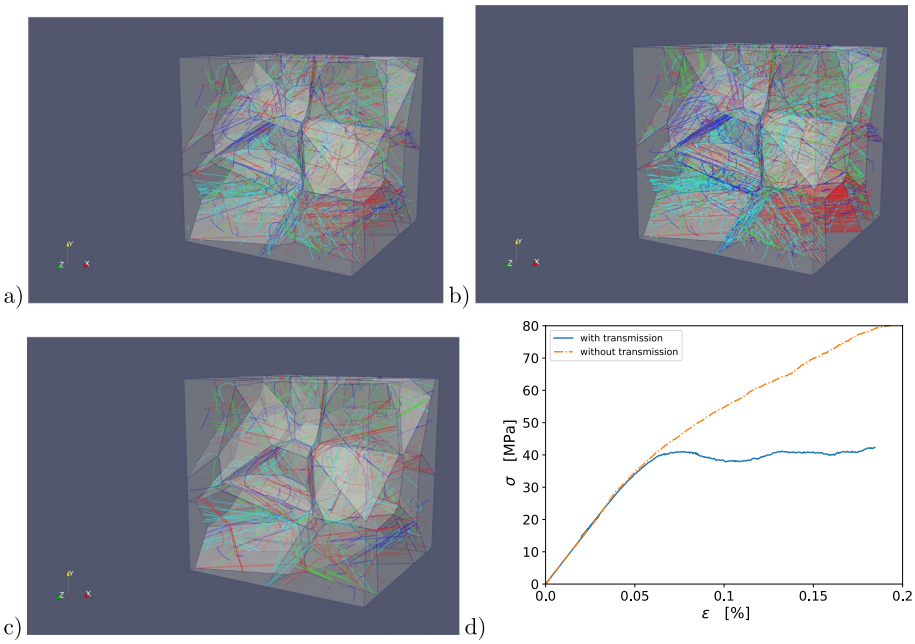

Fig. 7 Polycrystal with 40 grains and random orientations: Dislocations are colored according to their glide plane normal. In a) and b) dislocation transmission is allowed and many residual dislocation lines are visible on the grain boundaries. The total strain in a) and b) is about 0.1 % resp. 0.18 %. The configuration in c) shows the dislocation structure for impenetrable grain boundaries (strain ≈ 0.1 %). Here, the formation of pile-ups towards the grain boundaries is observed. The effect of dislocation transmission on the stress-strain behavior is shown in d). For impenetrable grain boundaries, pronounced work hardening is observed. Allowing dislocation transmission leads to much lower and at the same time fluctuating flow stress

There, pile-ups are formed, which lead to strong work hardening evident in the macroscopic responses shown in d). With dislocation transmission, the flow stress oscillates around 40MPa, clearly a sign that transmission and thus plastification of neighboring grains is easy.

Discussion

Our model for explicit dislocation transmission in a mesoscale setting of discrete dislocation dynamics markedly improves upon existing ideas of dislocation-grain boundary interactions. Both extreme cases, without misorientation and the generic combined tilt/twist grain boundary high dislocation density contrast behave as expected. Since DDD is based on superposition, the two simple bicrystalline cases suffice to make the argument for upscaling and we demonstrate it with a 40-grain polycrystal.

Our model opens the path to direct comparisons with small-scale experiments of bicrystals, e.g. Imrich et al. (2014); Malyar et al. (2019), which will be done in the future. Experiments will further serve to calibrate our model with respect to including a stress resistance against dislocation transmission. The current limitation of the implementation is the requirement of flat grain boundaries which is not generally valid in polycrystalline settings. Another limitation is that the grain boundary itself can only move in a superposed/effective sense when the displacement fields of interfacial dislocations are summed up (Hu et al. 2009). However, this limitation is inherent to the DDD method

itself. A large strain formulation is not implemented but large (macroscopic) strains are anyway not within reach due to the associated computational costs.

Conclusion

We have presented an explicit model for the transmission of dislocation across grain boundaries in a mesoscale discrete dislocation dynamics framework. The choice for the outgoing glide system is based on a minimization of the glide plane normal and Burgers vector and a maximization of the outgoing resolved shear stress. Both the incoming and outgoing dislocations are coupled via a butterfly-shaped grain boundary dislocation which accounts for continuity across the boundary. Our examples validate the approach and similar simulations like the 40-grain polycrystal will be used in the future for direct comparison with experiments at the micrometer scale.

Acknowledgements
Partial financial support by the German Research Foundation (DFG) under contract number WE3544/5-2 through the research unit FOR1650 is gratefully acknowledged by both authors.

Authors' contributions
DW conceived the idea of the model. MS and DW jointly developed it further. MS implemented the model; DW refined the implementation. MS and DW wrote the main manuscript text. MS prepared Figs. 1, 2, 3, 4 and 5; DW prepared Fig. 6a-d. Both authors reviewed the manuscript.

Funding
Open Access funding enabled and organized by Projekt DEAL. This work was partially supported by the German Research Foundation (DFG) through the Research Unit FOR1650 ***Dislocation based plasticity*** under contract number WE3544/5-2.

Availability of data and materials
The data that support the findings of this study are available upon reasonable request from the authors.

Declarations

Competing interests
The authors declare no competing interests.

Received: 25 August 2023 Accepted: 2 May 2024
Published online: 24 May 2024

References

D.M. Barnett, J. Lothe, An image force theorem for dislocations in anisotropic bicrystals. J. Phys. F: Met. Phys. **4**, 1618–1635 (1974). https://doi.org/10.1088%2F0305-4608%2F4%2F10%2F010

E. Bayerschen, M. Stricker, S. Wulfinghoff, D. Weygand, T. Böhlke, Equivalent plastic strain gradient plasticity with grain boundary hardening and comparison to discrete dislocation dynamics. Proc. R. Soc. A. **471**, 20150388 (2015). https://doi.org/10.1098/rspa.2015.0388

T. Bieler, P. Eisenlohr, C. Zhang, H. Phukan, M. Crimp, Grain boundaries and interfaces in slip transfer. Curr. Opinion Solid State Mater. Sci. 18, 212–226 (2014). http://www.sciencedirect.com/science/article/pii/S1359028614000205. Slip Localization and Transfer in Deformation and Fatigue of Polycrystals

N.J. Burbery, R. Das, G. Po, N. Ghoniem, Understanding the threshold conditions for dislocation transmission from tilt grain boundaries in FCC metals under uniaxial loading. Appl. Mech. Mater. 553, 28–34 (2014) . Trans Tech Publications Ltd

N.B. Burbery, G. Po, R. Das, N. Ghoniem, W.G. Ferguson, Dislocation dynamics in polycrystals with atomistic-informed mechanisms of dislocation - grain boundary interactions. J. Micromech. Mol. Phys. 2, 1750003 (2017). http://www.worldscientific.com/doi/abs/10.1142/S2424913017500035

W. Cai, A. Arsenlis, C.R. Weinberger, V.V. Bulatov, A non-singular continuum theory of dislocations. J. Mech. Phys. Solids. 54, 561–587 (2006). https://www.sciencedirect.com/science/article/pii/S002250960500195X?via%3Dihub

J. Cho, J.C. Crone, A. Arsenlis, S. Aubry, Dislocation dynamics in polycrystalline materials. Model. Simul. Mater. Sci. Eng. **28**, 035009 (2020). https://doi.org/10.1088/1361-651x/ab6da8

M. Dewald, W.A. Curtin, Multiscale modeling of dislocation/grain-boundary interactions: Iii. 60° dislocations impinging on σ3, σ9 and σ11 tilt boundaries in al. Model. Simul. Mater. Sci. Eng. 19, 055002 (2011). https://doi.org/10.1088/0965-0393/19/5/055002

Y. Gao, Z. Zhuang, X. You, A hierarchical dislocation-grain boundary interaction model based on 3d discrete dislocation dynamics and molecular dynamics. Sci. China Phys. Mech. Astron. **54**, 625–632 (2011). https://doi.org/10.1007/s11433-011-4298-9

D. Gottschalk, A. McBride, B. Reddy, A. Javili, P. Wriggers, C. Hirschberger, Computational and theoretical aspects of a grain-boundary model that accounts for grain misorientation and grain-boundary orientation (2015). arXiv:1505.01822v1

Y. Guo, T. Britton, A. Wilkinson, Slip band–grain boundary interactions in commercial-purity titanium. Acta Mater. 76, 1–12 (2014). http://www.sciencedirect.com/science/article/pii/S1359645414003632
E.O. Hall, The deformation and ageing of mild steel: III discussion of results. Proc. Phys. Soc. Sect. B. 64, 747–754 (1951). http://stacks.iop.org/0370-1301/64/i=9/a=303
Q. Hu, L. Li, N. Ghoniem, Stick–slip dynamics of coherent twin boundaries in copper. Acta Mater. 57, 4866–4873 (2009). https://www.sciencedirect.com/science/article/pii/S1359645409004042
D. Hull, D.J. Bacon, *Introduction to dislocations*, 4th edn. (Elsevier, 2011)
P.J. Imrich, C. Kirchlechner, C. Motz, G. Dehm, Differences in deformation behavior of bicrystalline cu micropillars containing a twin boundary or a large-angle grain boundary. Acta Mater. 73, 240–250 (2014). http://www.sciencedirect.com/science/article/pii/S1359645414002730
Z.H. Jin, P. Gumbsch, K. Albe, E. Ma, K. Lu, H. Gleiter, H. Hahn, Interactions between non-screw lattice dislocations and coherent twin boundaries in face-centered cubic metals. Acta Mater. 56, 1126–1135 (2008). https://www.sciencedirect.com/science/article/pii/S1359645407007768
M.d. Koning, R. Miller, V.V. Bulatov, F.F. Abraham, Modelling grain-boundary resistance in intergranular dislocation slip transmission. Philos. Mag. A. 82, 2511–2527 (2002). https://doi.org/10.1080/01418610208240050
J. Kacher, B. Eftink, B. Cui, I. Robertson, Dislocation interactions with grain boundaries. Curr. Opin. Solid State Mater. Sci. 18, 227–243 (2014). http://www.sciencedirect.com/science/article/pii/S1359028614000217. Slip Localization and Transfer in Deformation and Fatigue of Polycrystals
R. Kumar, F. Székely, E.V. der Giessen, Modelling dislocation transmission across tilt grain boundaries in 2d. Comput. Mater. Sci. 49, 46–54 (2010). http://www.sciencedirect.com/science/article/pii/S0927025610002314
B. Lagow, I. Robertson, M. Jouiad, D. Lassila, T. Lee, H. Birnbaum, Observation of dislocation dynamics in the electron microscope. Mater. Sci. Eng. A. 309, 445–450 (2001). http://www.sciencedirect.com/science/article/pii/S0921509300016993. Dislocations 2000: An International Conference on the Fundamentals of Plastic Deformation
T. Lee, I. Robertson, H. Birnbaum, Prediction of slip transfer mechanisms across grain boundaries. Scr. Metall. 23, 799–803 (1989). http://www.sciencedirect.com/science/article/pii/0036974889905346
J. Livingston, B. Chalmers, Multiple slip in bicrystal deformation. Acta Metall. 5, 322–327 (1957). http://www.sciencedirect.com/science/article/pii/0001616057900445
N. Malyar, B. Grabowski, G. Dehm, C. Kirchlechner, Dislocation slip transmission through a coherent σ3111 copper twin boundary: Strain rate sensitivity, activation volume and strength distribution function. Acta Mater. 161, 412–419 (2018). http://www.sciencedirect.com/science/article/pii/S1359645418307572
N.V. Malyar, H. Springer, J. Wichert, G. Dehm, C. Kirchlechner, Synthesis and mechanical testing of grain boundaries at the micro and sub-micro scale. Mater. Test. **61**, 5–18 (2019)
M. O'day, W. Curtin, A superposition framework for discrete dislocation plasticity. Trans. ASME-E-J. Appl. Mech. 71, 805–815 (2004)
N. Petch, The cleavage strength of polycrystals. J. Iron Steel Res. Inst. **174**, 25–28 (1953)
S.S. Quek, Z.H. Chooi, Z. Wu, Y.W. Zhang, D.J. Srolovitz, The inverse hall–petch relation in nanocrystalline metals: a discrete dislocation dynamics analysis. J. Mech. Phys. Solids. 88, 252–266 (2015). http://www.sciencedirect.com/science/article/pii/S0022509615303707
S.S. Quek, Z. Wu, Y.W. Zhang, D. J. Srolovitz, Polycrystal deformation in a discrete dislocation dynamics framework. Acta Mater. 75, 92–105 (2014). http://www.sciencedirect.com/science/article/pii/S1359645414003267
Z. Shen, R. Wagoner, W. Clark, Dislocation pile-up and grain boundary interactions in 304 stainless steel. Scr. Metall. 20, 921–926 (1986). http://www.sciencedirect.com/science/article/pii/0036974886904679
D.E. Spearot, M.D. Sangid, Insights on slip transmission at grain boundaries from atomistic simulations. Curr. Opinion Solid State Mater. Sci. 18, 188–195 (2014). http://www.sciencedirect.com/science/article/pii/S1359028614000175. Slip Localization and Transfer in Deformation and Fatigue of Polycrystals
M. Stricker, J. Gagel, S. Schmitt, K. Schulz, D. Weygand, P. Gumbsch, On slip transmission and grain boundary yielding. Mecanica. **51**, 271–278 (2015). https://doi.org/10.1007/s11012-015-0192-2
A.P. Sutton, R.W. Balluffi, *Interfaces in crystalline materials*, 1st edn. Monographs on the physics and chemistry of materials, vol 51 (Clarendon Press, Oxford, 1996)
D. Weygand, L.H. Friedman, E.V. der Giessen, A. Needleman, Aspects of boundary-value problem solutions with three-dimensional dislocation dynamics. Model. Simul. Mater. Sci. Eng. 10, 437–468 (2002). http://stacks.iop.org/0965-0393/10/i=4/a=306
D. Weygand, P. Gumbsch, Study of dislocation reactions and rearrangements under different loading conditions. Mater. Sci. Eng. A. 400, 158–161 (2005). http://www.sciencedirect.com/science/article/pii/S0921509305003023
D. Weygand, J. Senger, C. Motz, W. Augustin, V. Heuveline, P. Gumbsch, in *High Performance Computing in Science and Engineering '08*, High performance computing and discrete dislocation dynamics: Plasticity of micrometer sized specimens (2009), pp. 507–523. https://doi.org/10.1007/978-3-540-88303-6_36
X. Zhang, S. Lu, B. Zhang, X. Tian, Q. Kan, G. Kang, Dislocation–grain boundary interaction-based discrete dislocation dynamics modeling and its application to bicrystals with different misorientations. Acta Mater. 202, 88–98 (2021). https://www.sciencedirect.com/science/article/pii/S1359645420308508
X. Zhang, K.E. Aifantis, J. Senger, D. Weygand, M. Zaiser, Internal length scale and grain boundary yield strength in gradient models of polycrystal plasticity: How do they relate to the dislocation microstructure? J. Mater. Res. **29**, 2116–2128 (2014)
C. Zhou, R. LeSar, Dislocation dynamics simulations of plasticity in polycrystalline thin films. Int. J. Plast. 30, 185–201 (2012). http://www.sciencedirect.com/science/article/pii/S0749641911001653
C. Zhou, R. LeSar, Dislocation dynamics simulations of the bauschinger effect in metallic thin films. Comput. Mater. Sci. 54, 350–355 (2012). http://www.sciencedirect.com/science/article/pii/S0927025611005398

Publisher's Note